Fracture Mechanics of Concrete Structures, de Borst et al (eds) © 2001 Swets & Zeitlinger, Lisse, ISBN 90 2651 825 0

Microstructural modeling of concrete using fracture and diffusion-based interface elements

C.M.López & J.Murcia
ICMAB-CSIC, Bellaterra (Barcelona), Spain
X.Mestre & I.Carol
ETSECCPB-UPC, Barcelona, Spain

ABSTRACT: The study of concrete behavior under mechanical and environmental actions is approached via microstructural analysis using the FEM. The discretization includes the larger aggregates embedded in a matrix which represents the mortar and the smaller aggregates. Zero-thickness interface elements representing potential crack lines are inserted along all aggregate-matrix boundaries, and also along the main lines of the matrix discretization. Mechanically speaking, these elements are equipped with a fracture-based constitutive law which constitutes a mixed-mode generalization of Hillerborg's "Fictitious Crack Model". Numerical results in pure tension and compression are presented showing a good qualitative agreement with well known behavior of concrete. Consideration of environmental actions requires a moisture diffusion analysis on the same meshes. The formulation of interface elements for diffusion analysis is also described and illustrated.

1 INTRODUCTION

The behavior of heterogeneous materials such as concrete is clearly determined by the microstructural geometry and properties. Macroscopic models of the continuum type, which have been used traditionally in structural analysis, may be realistic for simple loading scenarios. However, as loading cases become more complicated and, especially, as other phenomena such as diffusion of coupled behavior are important, accurate understanding of the material response can be drastically improved via microstructural analysis.

As recognized by several authors (Rots and Schellekens, 1990), zero-thickness interface elements with appropriate constitutive laws, provide the means of extending the FCM concept (Hillerborg et al., 1976) into a modern numerical analysis of fracture using the FEM. For a general crack propagation study in a homogeneous medium, this could require expensive remeshing. However, this technique seems especially appropriate for the microstructural analysis of heterogenous materials, in which a number of weak interfaces are already physically present within the material, and the remaining main potential crack paths can be easily established *a priori* of the analysis (Stankowski, 1990; Vonk, 1992).

Cracks and material interfaces may also constitute preferred ways for faster, localized moisture migration within the concrete. These may also be conveniently represented by zero-thickness interface elements, with an appropriate formulation within the context of a FE analysis of the non-linear diffusion problem. This analysis, especially in the prospect of coupled behavior, may be advantageously carried out on the same meshes as the mechanical analysis, with interfaces that may change their diffusion properties depending on mechanical crack opening.

In this paper, the on-going work along this line at ETSECCP-UPC is summarized. First, the meshes used for the 2-D analysis of concrete specimens are described in Sect.2. The fracture-based constitutive laws of the interfaces for mechanical analysis are described in Sect.3. Some results obtained in the analysis of concrete specimens are described in Sect. 4. The formulation of the zero-thickness interface for diffusion analysis is then summarized in Sect.5. Some concluding remarks are finally presented in Sect. 6.

2 GEOMETRIC ASPECT OF INTERFACE ELEMENTS, DISCRETIZATION OF CONCRETE SPECIMENS

The interface elements used are "zero-thickness" isoparametric elements that can be inserted in between standard continuum finite elements. The nodes are grouped in pairs, which match on each side those of the adjacent elements. The two nodes from each pair are normally assigned the same coordinates, although they may also be given slightly separate locations if needed to represent some thickness or filling present in a physical interface.

Square concrete specimens of 14x14 cm dimensions, which include 4x4 and 6x6 arrangements of irregular aggregates are discretized using normal continuum elements. Then, a number of zero-thickness interface elements are inserted along the aggregate-matrix interface, and also across the mortar matrix, to allow for the most relevant failure mechanisms.

The geometry of the aggregates was taken from previous numerical work by Stankowski (1990), who generated these geometries using Voronoi/Delaunay theory on a perturbed mesh of initially regularly-spaced points. For our purposes, the aggregate geometry was preserved, but the FE mesh was completely rebuilt in order to provide straighter crack paths, following the ideas proposed by Vonk (1992).

In Figs. 1a and 1b, the discretization used for the matrix and the aggregate parts of the mesh for the 6x6 specimen are shown separately. Fig. 1c shows the interface lines in the same mesh, and figure 1d depicts a detail of node arrangements in pairs and interface intersections.

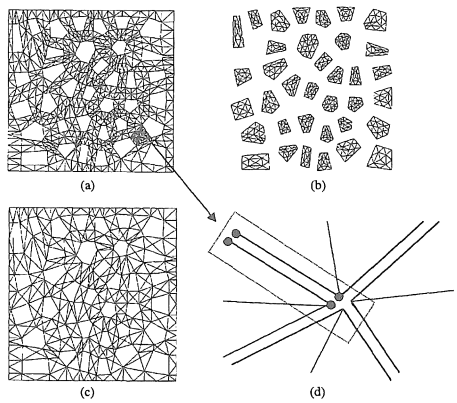

Figure 1. FE discretization of the 6x6 arrangement: a) matrix, b) aggregates, c) interfaces inserted, and d) details of discretization.

3 INTERFACE MODEL FOR MECHANICAL ANALYSIS

Interface behavior is formulated in terms of the normal and shear components of stresses (tractions) on the interface plane, $\sigma = [\sigma_N, \sigma_T]^t$, and corresponding relative displacements $\mathbf{u} = [u_N, u_T]^t$ (t = transposed). The constitutive model is analogous to that used for each potential crack plane in the multicrack model (Carol & Prat, 1995); it has been recently described in detail and compared to other existing interface models in Carol et al. (1997) and López (1999), and its main features and verification are summarized in the following.

The constitutive formulation conforms to work-softening elasto-plasticity, in which plastic relative displacements can be identified with crack openings. The main features of the plastic model are represented in Fig. 2. The initial loading (failure) surface $F = 0$ is given as a three-parameter hyperbola (tensile strength χ, asymptotic "cohesion" c, and asymptotic friction angle $\tan\phi$, Fig. 2a). Classic Mode I fracture occurs in pure tension. A second Mode IIa is defined under shear and high compression, with no dilatancy allowed (Fig. 2b). The fracture energies G_f^I and G_f^{IIa} are two model parameters. After initial cracking, χ, c and $\tan\phi$ decrease (Figs. 2d and 2e), and the loading surface shrinks, degenerating in the limit case into a pair of straight lines representing pure friction (Fig. 2c). The process is driven by the energy spent in fracture process, W^{cr}, the increments of which are taken equal to the increments of plastic work, less frictional work in compression. Total exhaustion of tensile strength ($\chi = 0$) is reached for $W^{cr} = G_f^I$, and residual friction ($c = 0$ and $\tan\phi = \tan\phi_r$) is reached for $W^{cr} = G_f^{IIa}$. Additional parameters α_χ, α_c and α_ϕ allow for different shapes of the softening laws (linear decay for $\alpha_\chi = \alpha_c = \alpha_\phi = 0$, see Figs.2d, 2e).

The plastic model is fully associated in tension ($Q = F$), but not in compression, where dilatancy is reduced with normal stress σ_N (vanishing for $\sigma_N \rightarrow \sigma^{dil}$, which is an additional parameter of the model) and also with shear degradation measured by c/c_0 (vanishing for $c \rightarrow 0$, i.e. for $W^{cr} \rightarrow G_f^{IIa}$). The dilatancy decay functions also include shape parameters α_σ^{dil} and α_c^{dil} (also linear decay for zero values of shape parameters). The elastic stiffness matrix is diagonal with constant K_N and K_T, which can be regarded simply as penalty coefficients.

Overall, the model has the following 8 required parameters: elastic K_N and K_T, initial strength χ_0, c_0, $\tan\phi_0$, fracture energies G_f^I, G_f^{IIa} and zero-dilatancy stress σ^{dil}, plus the residual friction angle $\tan\phi_r$ (which can be set equal to $\tan\phi_0$ in the absence of specific information) and the five shape parameters α_χ , α_c , α_ϕ , α_σ^{dil} and α_c^{dil} (which can all be set to zero in the absence of specific information).

The element formulation for mechanical analysis follows standard procedures based on the Principle of Virtual Work. The only special consideration refers to the integration rules which correspond to Newton-Cotes/Lobatto schemes (with integration points in between each pair of nodes) in order to avoid spurious oscillations in the resulting stress profiles. See more details in Gens et al. (1990). More details about numerical and computational techniques used can be found in Carol et al. (2001).

The interface model is implemented the finite element code DRAC (Prat et al., 1993). This is a research-oriented geotechnical/structural FE program with 2D/3D capabilities, various element types including interfaces, post-processing module DRAC-VIU, diffusion analysis module DRACFLOW, all in-house developed at the Dept. of Geotechnical Engineering and Geo-Sciences of ETSECCPB-UPC.

4 EXAMPLES OF MICROSTRUCTURAL FRACTURE ANALYSIS

4.1 *Uniaxial tension*

A prescribed tensile displacement is applied to one side of the specimen, leaving lateral displacement free in the transverse direction. Sum of reactions divided by the size of the specimen gives the average applied stress.

The material parameters are: E = 70000 MPa (aggregate), E = 25000 MPa (mortar) and ν = 0.18 (both) for the continuum elements; for the aggregate-

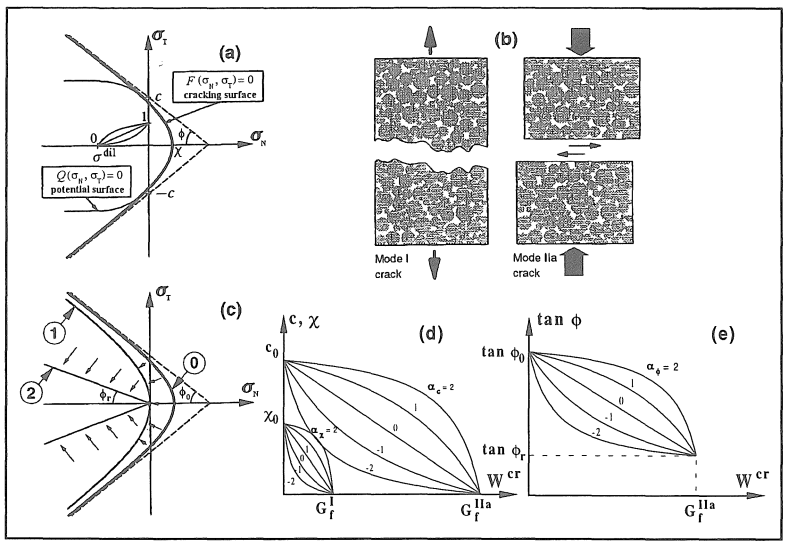

Figure 2. Crack laws: (a) hyperbolic cracking surface F and plastic potential Q; (b) fundamental modes of fracture; (c) evolution of cracking surface; (d) softening laws for χ and c and (e) softening law for tanϕ.

mortar interfaces: $K_N = K_T = 10^9$ MPa/m, tanϕ_0 = tanϕ_r = 0.8, tensile strength χ_0 = 3 MPa, c_0 = 4.5 MPa, G_f^I = 0.03 N/mm, $G_f^{IIa} = 10G_f^I$, σ^{dil} = 7 MPa, and all other parameters equal to zero; for the mortar-mortar interfaces the same parameters except for χ_0 = 6 MPa, c_0 = 9 MPa, G_f^I = 0.06 N/mm.

The calculations have been repeated with load applied in the x (horizontal) and y (vertical) directions for the 4x4 and 6x6 mesh, and the resulting average stress-average strain curves are represented in Fig. 3. It can be noted that all them yield similar results in spite of the relatively different geometries involved.

Fig. 4 includes results of the 4x4 specimen loaded vertically, at three different stages of the loading sequence (points Y_1, Y_2 and Y_3 in Fig. 3), as well as the final deformed mesh (magnification factor = 200). The thickness of the lines represents the amount of energy spent in the fracture process (W^{cr}) at each point of the interface.

It is apparent that many cracks start developing initially, but at some point deformations localize in one or two cracks perpendicular to the applied load, that develop while all other cracks unload (indicated with arrows in figure 4c). Well-known phenomena such as crack bridging and branching may be observed in the results.

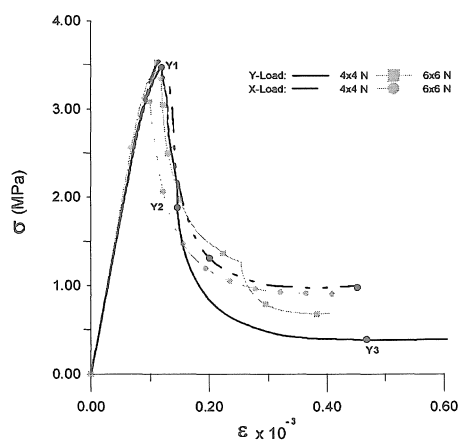

Figure 3. Average stress-strain curves in uniaxial tension.

4.2 *Uniaxial compression*

In this case, load is also applied *via* uniform prescribed displacement on the top side of the specimen, while lateral displacements are allowed. The material parameters are E = 70000 MPa (aggregate), E = 25000 MPa (mortar) and ν = 0.2 (both); for the aggregate-mortar interfaces: $K_N = K_T = 10^9$ MPa/m, tanϕ_0 = 0.6, χ_0 = 2 MPa, c_0 = 7 MPa, G_f^I = 0.03 N/mm, $G_f^{IIa} = 10G_f^I$, σ^{dil} = 40 MPa, tanϕ_r = 0.2, α_σ^{dil} = -2, α_ϕ = 1, and all other parameters equal to zero; for the mortar-mortar interfaces the same parameters except for χ_0 = 4 MPa, c_0 = 14 MPa, G_f^I = 0.06 N/mm.

In Fig. 5, the stress-strain curves obtained with the 4x4 and the 6x6 meshes are plotted. The vertical axis represents the average applied stress and the right side of the horizontal axis represents the corresponding (prescribed) strain, while the left side of the horizontal axis represents average lateral strain. It is apparent that the results obtained with both meshes are quite similar, and they agree well with the typical behavior of concrete in uniax-

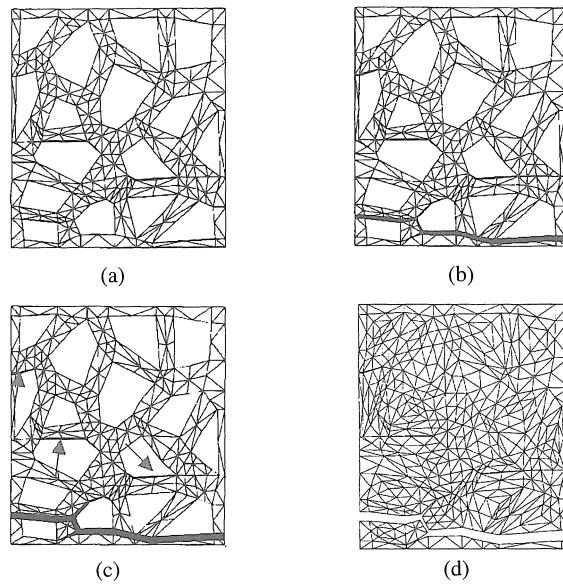

Figure 4. Progressive cracking of the 4x4 mesh in uniaxial tension (a, b, c) represented by amount of energy spent, and final deformed mesh (d) upon *y* loading.

ial compression as observed in experiments (Van Mier, 1984, 1997).

In the left part of the figure, one can see the evolution of the lateral strain. Initially, ε_2 evolves maintaining approximately the Poisson relation. Before reaching the peak load, the lateral strain starts growing faster, and in the softening branch it overcomes the strain prescribed in the loading direction. In Fig. 6, the same behavior is represented in terms of a "volumetric" strain defined as $(\varepsilon_1+2\varepsilon_2)$, which also matches the typical experimental curves.

In Fig. 7, the evolution of the cracking process of the 6x6 specimen is represented in terms of the modulus of the "plastic" (cracking) part of the relative displacement vector at each point of the interfaces. The four stages of loading represented in the figure, correspond to the four points marked 1, 2, 3 and 4 on the stress-strain curves of Fig. 5.

The state represented in figure 7a corresponds to point 1 with widespread distributed microcracks mainly originated at the concrete-mortar interface. Fig. 7b corresponds to point 2, in which the localization process has started. Some of the microcracks are getting connected sideways forming inclined macrocracks, while the rest unload. At point 3 (Fig. 7c), one can clearly appreciate one or two localization bands well developed which divide the specimen into three main blocks, while the remaining incipient macrocracks have arrested.

In the final stage (Fig. 7d, point 4 in Fig. 5) the same scheme is maintained, and the few blocks formed slide with friction with respect to each other. Note that the transition from 7b to 7c represents a significant reduction of stress (points 2 to 3 in Fig. 5).

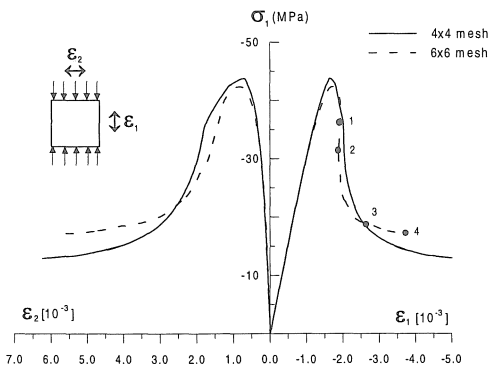

Figure 5. Average stress-strain curves for the 4x4 and 6x6 meshes under uniaxial compression.

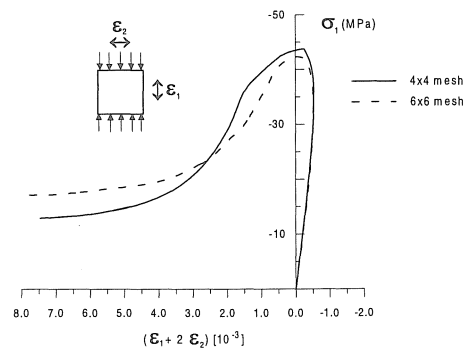

Figure 6. Stress vs. "fictitious" volumetric strain curves in uniaxial compression.

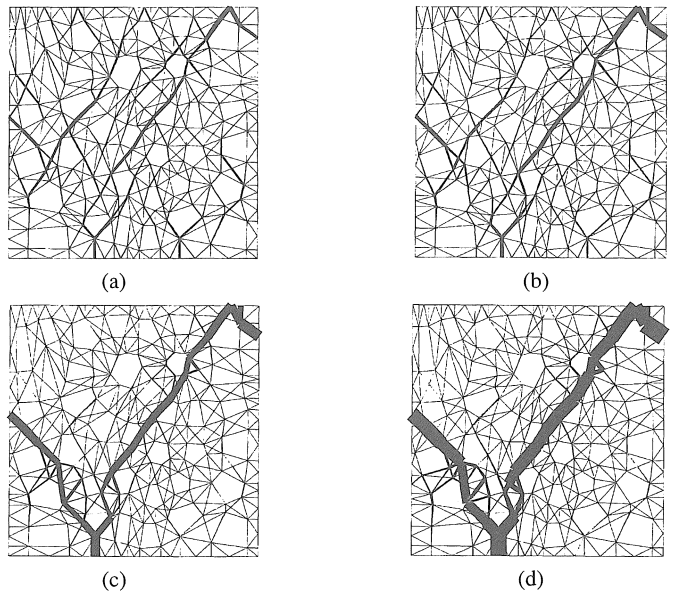

Figure 7. Localization process in uniaxial compression, represented in terms of the magnitude of plastic strain at the interfaces.

5 DIFFUSION ANALYSIS WITH INTERFACES

The diffusion analysis with interfaces is based on the well-known differential equation:

$$\frac{\partial}{\partial x_i}\left[D\frac{\partial H}{\partial x_i}\right]+h(x)=\frac{\partial H}{\partial t} \qquad (1)$$

Finite Element techniques for this equation are well established, see for instance Zienckiewic (1977). For the specific problem of moisture diffusion in concrete, the equation is written most advantageously in terms of the relative humidity H, as proposed by Bazant and Najjar (1971). Relative humidity therefore becomes the nodal variable for the FE analysis. Diffusivity is generally accepted to depend on relative humidity, i.e. D=D(H), which gives the problem a non-linear character and requires iterative procedures (Alvaredo and Wittmann, 1992).

In order to achieve a fully coupled analysis, the diffusion analysis must be run on the same meshes as the mechanical calculations. This means to develop interface elements with double nodes, also for the diffusion analysis, which seems not standard in the literature of other fields with similar equations. For instance, in flow in porous media, localized flow in cracks is usually represented by single-noded line elements (in 2-D) or surface elements (in 3-D) which are simply superposed to the standard continuum field. If double-node interface elements are considered, the nodes on each side of the interface may give different values of H. This means that the interface elements in this case represent not only preferential flow channels, but also discontinuities in the potential field.

In order to formulate these elements, two different mechanisms are taken into account: the longitudinal and the transversal flow. For each of them, separate interface diffusivities, K_L and K_T, are postulated. The longitudinal flow is treated as a conventional problem of diffusion through a line (in 2D) or surface (in 3D). This flow is formulated in terms of variables at the "mid-points" of the interface, which are points located at mid-distance between each pair of nodes. This leads to a first element matrix equation restricted to the mid-point variables, which involves a "longitudinal stiffness matrix" $\mathbb{K}_{PM,L}$.

The transversal flow is treated in a different way, more similar to the traditional mechanical behavior of interfaces. In this case, the PVW is applied to obtain a second matrix element equation, also restricted to mid-point variables, although in this case representing jumps. This equation involves a "transversal stiffness matrix" $\mathbb{K}_{PM,T}$.

Finally, both mechanisms are combined, assuming that, at the mid-point, H is the average of the values at the corresponding pair of interface nodes, and that longitudinal and transversal flows at the interface nodes sum effects in a consistent way (Mestre, 1999). This leads to the final matrix equation of the interface element involving all double nodes:

$$\mathbb{Q}_J = \mathbb{K}_J \cdot \mathbb{H}_J \qquad (2)$$

where $\mathbb{Q}_J$ and $\mathbb{H}_J$ are the full nodal flow ("force") and H ("displacements") vectors, and $\mathbb{K}_J$ is the global interface "stiffness" matrix which has the following structure:

$$\mathbf{K}_J = \begin{bmatrix} \frac{1}{4}\mathbf{K}_{PM.L} + \mathbf{K}_{PM.T} & \frac{1}{4}\mathbf{K}_{PM.L} - \mathbf{K}_{PM.T} \\ \frac{1}{4}\mathbf{K}_{PM.L} - \mathbf{K}_{PM.T} & \frac{1}{4}\mathbf{K}_{PM.L} + \mathbf{K}_{PM.T} \end{bmatrix} \quad (3)$$

A first verification example of this formulation involves a band of material with a longitudinal interface. Dimensions are 6x2 cm. Variable H is prescribed to 1 on the right end, no flow is allowed on the upper and lower boundaries, and the flow is also prevented on the left boundary, except for the interface opening, where H is set to zero. The diffussivity of the continuum is considered constant D=1cm/s. The interface diffusivities are $K_L=10^4 cm^2/s$ and $K_T=10^6 cm/s$. Although originally intended as a purely academic example, this could represent for instance a crack and the surrounding material, in a regularly-spaced arrangement of parallel cracks in a large concrete element. The fact that the flow is allowed only to exit the domain through the crack mouth could correspond for instance to a sealing coating or lining, which has only been broken by the cracks.

Fig.8 shows the steady state results of the diffusion analysis with interfaces, as a contour plot of the values of the potential variable H. Although not explicitly represented, the flow directions are also implied by the direction perpendicular to the equipotential lines at each point of the domain. (even if the interface has no thickness, it has been plotted with a small value for representation purposes).

It can be observed that the flow is initially horizontal (right side of specimen) and then progressively converges into the interface, which is the only exit point on the left side.

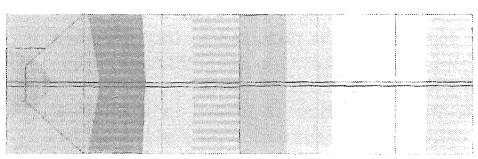

Figure 8. Example of diffusion analysis with interfaces. H on the right side is prescribed to 1, on the left interface mouth to 0. Each band corresponds to a 0.1 drop in the potential.

6 CONCLUDING REMARKS

Some aspects of the on-going research work at ETSECCPB-UPC on microstructural analysis of concrete have been described. The model for concrete fracture is based on "zero-thickness" interface elements equipped with a fracture-based constitutive law. These interface elements are inserted between standard continuum elements with elastic behavior, and represent potential crack lines embedded in the mesh. The constitutive law has the structure of work-softening elasto-plasticity, with two parameters, which represent fracture energies in models I and IIa.

The microstructural model proposed can represent some of the most salient features of experimental concrete fracture, such as microcracking, localization and macroscopic crack formation, both in tension and compression. Other loading cases such as Brazilian, tension/compresion, etc. can be found in Lopez (1999). A qualitative agreement with well known concrete behavior is obtained on the average stress-strain curves as well as in the microcrack patterns and their coalescence and evolution. This type of model also opens the possibility to study the influence of aggregate shape and size, relative strengths of aggregate-matrix, aggregate-aggregate and matrix-matrix interfaces, and a number of other effects impossible to account for using macroscopic models.

Finally, some attention in the paper has been devoted to the diffusion analysis with interfaces, which is needed in order to study a number of coupled problems of great interest such as shrinkage cracking, penetration of ambient agents or water related to durability aspects, and hydraulic fracture. The formulation of the interface element for diffusion analysis has been outlined, and a first simple verification example presented. Work is currently under way to integrate all these capabilities in to a single tool of general coupled analysis of concrete under combined mechanical and environmental actions.

ACKNOWLEDGEMENTS

The authors wish to thank MCYT (Madrid, Spain) for the support received through research projects MAT2000-1007, and Schlumberger for its Stitching Fund grant to the fourth author in 2000. The first author also wants to acknowledge the support received from Generalitat de Catalunya (Barcelona, Spain), through Conselleria d'Obres Públiques and Direcció General de Recerca (project, GRQ 99-00135), and from CSIC (Madrid, Spain) through a post-doctoral fellowship co-sponsored by Electricite de France.

REFERENCES

Alvaredo, A.M. and Wittmann, F. H. (1992). Crack formation due to hygral gradients. In: Z.P. Bazant, editor, Fracture Mechanics of Concrete Structures (Proceedings FRAMCOS-1), Elsevier. pp. 960-966.

Bazant, Z.P. & Najjar, L.J. (1971). Drying of concrete as a nonlinear diffusion problem. *Cement and Concrete Research,* vol.1, pp. 461-473.

Carol, I. & Prat, P.C. (1995). A multicrack model based on the theory of multisurface plasticity and two fracture energies. In Owen, D.R.J., Oñate, E., and Hinton, E., editors, *Computational plasticity* (COMPLAS IV), Vol. 2 pp.1583-1594, Barcelona, Pineridge Press.

Carol, I., Prat, P.C. and López, C.M. (1997). A normal/shear cracking model. Application to discrete crack analysis. *J. of Engineering Mechanics.* Vol. **123**,No 8.

Carol, I., López, C:M. and Roa, O. (2001). Micromechanical analysis of quasi-brittle materials using fracture-based interface elements. *Int. J. of Numerical Methods in Engineering*. (Accepted).

Gens, A., Carol, I. and Alonso, E. (1990). A constitutive model for rock joints. Formulation and numerical implementation. *Computers and Geotechnics*, 9:3-20.

Hillerborg, A., Modéer, M. and Petersson, P.E. (1976). Analysis of crack formation and crack growth in concrete by means of Fracture Mechanics and Finite Elements. *Cement and Concrete Research*, 6(6):773-781.

López, C.M. (1999). *Microstructural analysis of concrete fracture using interface elements. Application to various concretes* (In Spanish). Doctoral Thesis. Universitat Politecnica de Catalunya. ETSECCCP-UPC, E-08034 Barcelona, Spain.

Mestre, X. (1999). *A study of flow in porous media using the FEM, with interface elements in 3D.* Graduation thesis ETSECCPB-UPC.

Prat, P.C., Gens, A., Carol, I., Ledesma, A. and Gili, J.A. (1993). DRAC: A computer software for the analysis of rock mechanics problems. In H. Liu, editor, *Application of computer methods in rock mechanics*, 2: 1361 - 1368, Xian, China. Shaanxi Science and Technology Press.

Rots, J.G. and Schellekens J.C.J. (1990). Interface elements in concrete mechanics. In: Bicanic, N. and Mang, H., editors, *Computer-Aided Analysis and Design of Concrete Structures.* (proc. SCI-C). Pineridge Press, pp. 909—918.

Stankowski, T. (1990). *Numerical simulation of progressive failure in particle composites.* PhD thesis, Dept. CEAE, University of Colorado, Boulder, CO 80309-0428, USA.

van Mier, J. G. M. (1984). *Strain-softening of Concrete under Multiaxial Loading Conditions.* PhD thesis, Eindhoven University of Technology, Eindhoven, The Netherlands.

van Mier, J. G. M. (1997). *Fracture Processes of Concrete.* CRC Press.

Vonk, R. (1992). *Softening of concrete loaded in compression.* PhD thesis, Technische Universiteit Eindhoven, Postbus 513, 5600 MB Eindhoven, Netherlands.

Zienkiewicz, O.C. (1977). *Finite Element Method.* 3rd ed. McGraw-Hill.